

Signatures of two-body random matrix ensembles in Sm I

Dilip Angom and V. K. B. Kota

Physical Research Laboratory, Navarangpura, Ahmedabad-380 009, India

(Received 25 October 2002; published 28 May 2003)

Configuration interaction calculations for the Sm I $J=0^+$ and 4^+ with matrix dimensions 1351 and 7325 are carried out. The eigenvalues and eigenfunctions are analyzed for density of states, strength functions, and information entropy in wave functions and compared with the Gaussian forms given by two-body random matrix ensembles (TBRE). Signatures of TBRE are clearly seen in the Sm I example.

DOI: 10.1103/PhysRevA.67.052508

PACS number(s): 32.30.-r, 05.30.-d, 05.45.Mt, 32.10.-f

Canonical random matrix theory (RMT) defined by Gaussian orthogonal (GOE), unitary, and symplectic ensembles applies to a wide variety of quantum systems such as nuclei, atoms, molecules, quantum dots, etc. [1]. Very early, Rosenzweig and Porter [2], and Camarda [3] analyzed atomic energy level data for the nearest-neighbor spacing distribution (NNSD) and Dyson-Mehta $\bar{\Delta}_3$ statistic, and established that GOE describes the local level fluctuations in atoms. More recently, this was further confirmed by large configuration interaction calculations of atomic spectra of Ce I and Pr I by Flambaum *et al.* [4,5] and Cummings *et al.* [6]. In addition to the level statistics, they also confirmed the operation of the Porter-Thomas form (given by GOE) for strength fluctuations. Although GOE applies for fluctuations, in a pioneering paper Flambaum *et al.* [4] pointed out, by studying Ce I in detail, quantities such as strength functions [$F_k(E)$] and information entropy [$S^{\text{info}}(E)$] or equivalently the number of principal components [$(NPC)_E$] are most important ingredients of an interacting many particle system; $F_k(E)$, $S^{\text{info}}(E)$, and $(NPC)_E$ are defined later, and also note that strength functions and occupation numbers determine transition strengths. At this stage, it should be pointed out that GOE implies that the interaction is m body for a m particle system. However, for systems such as atoms, the interaction is essentially a mean-field one body plus a complexity generating two-body interaction. As a result of this, the m particle Hamiltonian matrix becomes a sparse matrix (many matrix elements are zero due to two-body selection rules). By examining the Ce I Hamiltonian matrix (for $J=4^-$ and $J=4^+$), Flambaum *et al.* invoked banded random matrices to describe the calculated $F_k(E)$ and $S^{\text{info}}(E)$. A more detailed numerical study of this type was carried out recently by Cummings *et al.* [7], and they considered Ce I and Pr I with ls and jj couplings. On the other hand, it is well known from the structure studies of atomic nuclei that for an interacting particle system with sufficiently large number of particles ($m \geq 6$), two-body random matrix ensembles (TBRE) describe $F_k(E)$, $S^{\text{info}}(E)$, transition matrix elements, etc. [8]. TBRE is also called embedded GOE of two-body interactions or simply EGOE(2). With one plus two-body interactions, one has in fact EGOE(1+2). In addition to nuclei, EGOE(1+2) is shown to describe some properties of quantum dots and small metallic grains [9,10]. They are also used in the discussion of operability of quantum computers [11]. With these, it is natural to expect that TBRE or

EGOE(1+2) also applies to atoms. In order to probe into this question, in this paper, we studied the structure of Sm I eigenfunctions structure in terms of $F_k(E)$ and $S^{\text{info}}(E)$.

Rare earth elements are chosen in the studies, investigating the signatures of RMT in atomic systems as these have very complicated spectra due to the large number of valence electrons in partially filled $4f$ valence shell and other close lying electronic shells. The atomic Sm I used in the present study has 62 electrons of which eight are in the valence shells $4f$ and $6s$, which can be treated as active. Hence, Sm I is a better candidate to test the general properties of TBRE compared to Ce I and Pr I, which have only four and five active electrons each. The ground state of Sm I is $4f^6 6s^2 {}^1S_0$. The Dirac-Coulomb Hamiltonian is used in the present study as it is an appropriate choice for high- Z atom such as Sm. The Dirac-Coulomb Hamiltonian of an N electron atom is

$$H^{\text{DC}} = \sum_{i=1}^N \left(c \boldsymbol{\alpha}_i \cdot \mathbf{p}_i + c^2 (\beta_i - 1) - \frac{Z(\mathbf{r}_i)}{r_i} \right) + \sum_{i>j}^{N,N} \frac{1}{|\mathbf{r}_i - \mathbf{r}_j|}, \quad (1)$$

where $\boldsymbol{\alpha}_i$ and β_i are the Dirac matrices, \mathbf{p}_i is the linear momentum of the electron, $Z(\mathbf{r}_i)$ is the effective nuclear charge at \mathbf{r}_i , and the last term is the electron-electron coulomb interaction. It is to be noted that all the calculations with Eq. (1) are in atomic units, where $\hbar = 1$, $m_e = 1$, and $e = 1$. The occupied orbitals $(1-6)s_{1/2}$, $(2-5)p_{1/2}$, $(2-5)p_{3/2}$, $(3-4)d_{3/2}$, $(3-4)d_{5/2}$, and $4f_{5/2}$ are generated by a self-consistent Dirac-Fock calculation of the configuration $4f_{5/2}^6 6s_{1/2}^2$. The orbitals are frozen, and $6p_{1/2}$, $6p_{3/2}$, $5d_{3/2}$, $5d_{5/2}$, and $4f_{7/2}$ are generated by a sequence of Dirac-Fock calculations of the configuration $4f_{5/2}^6 6s_{1/2} \psi$, where ψ is the orbital to be generated. Using the orbitals, a basis set of configuration state functions (CSF's) $\{|\Phi_k\rangle\}$ is constructed. A configuration interaction (CI) calculation within the CSF space generates a set of atomic state functions (ASF) $\{|\Psi_E\rangle\}$, each of the ASF is a linear combination of the CSF's $|\Psi_E\rangle = \sum_k C_k^E |\Phi_k\rangle$ and are eigenfunctions of the Dirac-Coulomb Hamiltonian. The Dirac-Fock calculations are done using the multiconfiguration Dirac-Fock code GRASP92 [12], which is a relativistic adaptation of the multi-configuration Hartree-Fock (MCDF) [13]. Previous calculations of Sm I properties such as lifetime, excitation energies, and hyperfine constants are compared with the experimental

data [14], and established that method of calculations such as the present one can describe Sm I.

The configurations considered in our calculation are generated by all possible single and double excitations from $4f^6 6s^2$ to the $5d$ and $6p$ orbitals. The possible even parity configurations in nonrelativistic notations are $4f^6 6s 5d$, $4f^5 6s^2 6p$, $4f^6 5d^2$, $4f^6 6p^2$, $4f^5 6s 5d 6p$, $4f^4 6s^2 5d^2$, and $4f^4 6s^2 6p^2$. The CSF's having $J=0^+, 4^+$ within this configuration space are considered and two separate CI calculations are done. The number of relativistic CSF's are 1351 and 7325 for $J=0^+$ and $J=4^+$, respectively and eigen spectra have a span of 2.65 hartree and 2.46 hartree, respectively, where the span is the difference between the lowest and the highest eigenvalue. Hereafter, the number of the CSF's or the dimension of the Hamiltonian matrix is referred to as d . The energy span shows that $J=4^+$ has a denser spectra as a consequence of the larger number of relativistic CSF's generated from each of the configuration. The centroids of the spectra located at 0.68 hartree for $J=0^+$ and 0.63 hartree for $J=4^+$ measured from the ground state, reflect the asymmetry of the density of states. Now we will turn to the statistical analysis of the eigenvalues and eigenfunctions in terms of EGOE. First let us briefly describe EGOE.

EGOE(k) for many (m) fermion systems is generated by defining the Hamiltonian H , which is, say, k body, to be GOE in k -particle space and then propagating it to m -particle spaces by using the geometry of the m -particle spaces. Here, one assumes that the m -particle space is a direct product space of single-particle states (say N in number), for example, as in the Sm I calculation. Now a EGOE(1+2) is defined by $\{H\} = [h(1)] + \{V(2)\}$, where $\{V(2)\}$ is EGOE(2) (say, with two particle matrix elements variance $|\langle a|ij|V(2)|kl\rangle|^2 = v^2$, where a means antisymmetrized) and $[h(1)]$ is a fixed one-body Hamiltonian (or an ensemble) with single-particle energies ϵ_i , $i=1, \dots, N$ having an average spacing Δ . With $\lambda = v/\Delta$, it is easily seen that EGOE(1+2) behaves as EGOE(2) as $\lambda \rightarrow \infty$. It is well known that for EGOE(2) in the dilute limit ($m \rightarrow \infty$, $N \rightarrow \infty$, and $m/N \rightarrow 0$), the ensemble averaged (smoothed) state densities $\rho^H(E)$ approach the Gaussian form [8,15]. Moreover, for EGOE(1+2) one can define two "quantum chaos" markers λ_c and λ_{F_k} so that for $\lambda > \lambda_c$, there is chaos in the sense that the level fluctuations start coming close to GOE fluctuations [16] and for $\lambda > \lambda_{F_k}$ (note that $\lambda_c < \lambda_{F_k}$) one has the Gaussian form not only for the smoothed state densities but also for the strength functions [17,18,8]. The $\lambda > \lambda_{F_k}$ region is called the Gaussian domain. Forms valid in this domain for $S^{\text{info}}(E)$ and $(NPC)_E$ are derived recently [17]. In the discussion ahead, no distinction is made between TBRE and EGOE(1+2) as we will be comparing Sm I calculations with the results valid in the Gaussian domain. It is to be noted that $\lambda_c \sim 1/m^2 N$ and $\lambda_{F_k} \sim 1/\sqrt{m}$, see Refs. [16] and [19], respectively. Therefore, it is easily seen that approach to the Gaussian domain will be faster with larger number m of active electrons. Our aim in this paper is to verify whether Sm I with $m=8$ is in the Gaussian domain.

The density of states $\rho^H(E)$ of the spectra exhibits a long tail in contrast to the TBRE prediction of a Gaussian. This

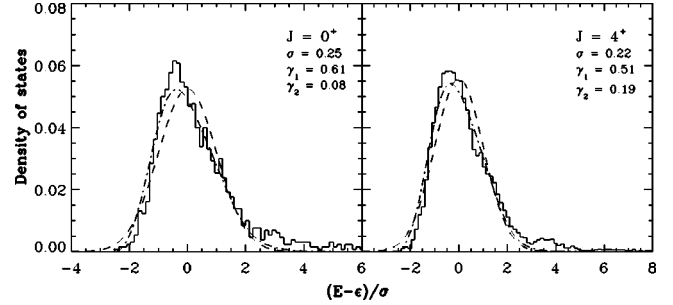


FIG. 1. Binned and normalized density of states (solid line); Gaussian calculated, neglecting the last few states (dashed line); and Edgeworth corrected Gaussian (dot-dashed line).

follows from the location of the centroids mentioned earlier. However, a Gaussian $\eta_G(\hat{E}) = (1/\sqrt{2\pi})\exp(-\hat{E}^2/2)$, where $\hat{E} = (E - \epsilon)/\sigma$ is the standardized variable characterized by the centroid ϵ and width σ of the $\rho^H(E)$, after neglecting the last few states matches well with the CI results as shown in Fig. 1. Note that $\rho^H(E)dE = \eta(\hat{E})d\hat{E}$. The $\eta_G(\hat{E})$ can further be refined to an Edgeworth corrected Gaussian [8,20]

$$\eta_{\text{ED}}(\hat{E}) = \eta_G(\hat{E}) \left\{ 1 + \frac{\gamma_1}{6}\text{He}_3(\hat{E}) + \frac{\gamma_2}{24}\text{He}_4(\hat{E}) + \frac{\gamma_1^2}{72}\text{He}_6(\hat{E}) \right\}, \quad (2)$$

where $\text{He}_r(\hat{E})$ are Hermite polynomials, and γ_1 and γ_2 are skewness and excess, respectively. In generating Fig. 1, these are calculated using the definitions $\gamma_1 = \langle (E - \epsilon)^3 \rangle / \sigma^3$ and $\gamma_2 = \langle (E - \epsilon)^4 \rangle / \sigma^4 - 3$. The shift of the $\eta_{\text{ED}}(\hat{E})$ peak reflects the asymmetry of $\rho^H(E)$, which may be partly due to the limited excitations from the valence shells. Figure 1 shows that bulk of the spectrum is well represented by the Edgeworth corrected Gaussian and this is quite different from the Wigner's semicircle of the canonical RMT [1]. It should be mentioned that TBRE has ergodic eigenstates in the middle of its spectrum but there could be deviations at the edges [21]. Gaussian like density of states was also observed in the Sm IX spectra by O'Sullivan *et al.* [22].

The strength functions or local density of states $F_k(E) = \sum_{E'} |C_k^{E'}|^2 \delta(E - E') = \overline{|C_k^E|^2} \rho(E)$ for EGOE(1+2) undergoes a δ function \rightarrow Breit-Wigner (BW) \rightarrow Gaussian transition as λ makes a $0 \rightarrow \lambda_c \rightarrow \lambda_{F_k}$ transition [8,18]. The $F_k(E)$ centroid $\epsilon_k = \langle \Phi_k | H | \Phi_k \rangle$ and variance $\sigma_k^2 = \langle \Phi_k | H^2 | \Phi_k \rangle - \epsilon_k^2$. The BW form is defined by the Lorentzian $(1/2\pi)\Gamma / [(E - \overline{E}_k)^2 + \Gamma^2/4]$, where Γ is the spreading width and \overline{E}_k is the centroid. The $\rho^H(E)$ being close to the Gaussian except for the tails (also level statistics following GOE as shown in Fig. 3 ahead) it is to be expected that the $F_k(E)$'s should follow the Gaussian form for the middle CSF's. This result is tested in Fig. 2. For example, with $k=3000$ and 3300 for $J=4^+$ shows that the Gaussian features are more prominent in $F_k(E)$'s of medium energy CSF's. A closer examination of the tail part and the central portion of the calculated $F_k(E)$'s, shown in Fig. 2 clearly points out that the Lorentzian will not give a good fit. This is unlike the case with Ce I [4] and Pr I [7] which do not have sufficient

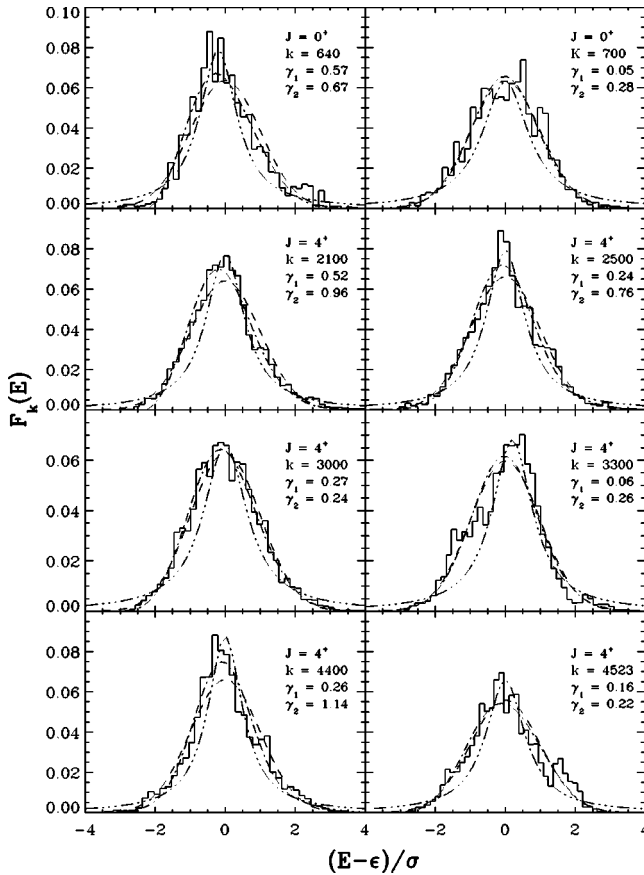


FIG. 2. $F_k(E)$ of selected CSF's; k denotes the CSF number. The dashed, dot-dashed, and dot-dot-dot-dashed curves are the Gaussian, Edgeworth corrected Gaussian, and Lorentzian, respectively.

number of active electrons for the Gaussian form to operate. Typically, $\sigma_k \sim 0.12$ hartree in contrast to $\Gamma \sim 0.18$ hartree for $J=4^+$, Γ is obtained by the Breit-Wigner fit. The Gaussian form of the $F_k(E)$'s of selected CSF's, shown in Fig. 2, brings out the action of TBRE in Sm I. However, it should be pointed out that the $F_k(E)$'s show multimodal structure, for example, the $J=4^+$ and $k=3300$ has two pronounced local maxima at $\hat{E} \sim -1$ and 0. As pointed by Flambaum *et al.* [4]

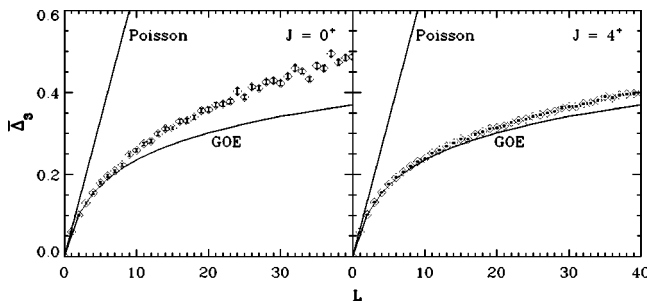


FIG. 3. Calculated $\bar{\Delta}_3(L)$ is compared with the Poisson and GOE values. To calculate $\bar{\Delta}_3(L)$, the cumulative number of energy states $N(E)$ are unfolded using the fourth order polynomial within selected region of the spectra; 30–800 and 170–5000 eigenvalues of the $J=0^+$ and $J=4^+$, respectively, are considered.

this could be due to the selection rules and nature of the two-body interaction. This will be investigated in detail elsewhere. Besides $F_k(E)$ one can also study the closely related function [17] that gives the spreading of the eigenfunctions, i.e., $|C_k^E|^2$ versus E_k [4,6]. Before going further, it should be added that the calculated nearest-neighbor spacing distribution and $\bar{\Delta}_3$ for the middle part of the spectrum follow GOE. Figure 3 shows the results for $\bar{\Delta}_3$. Gaussian densities with level fluctuations following GOE is a feature of EGOE(1+2) with $\lambda > \lambda_c$ [1,8]. In fact, even a noninteracting fermion system gives Gaussian level densities but with Poisson fluctuations. Finally, in indefinite spaces, in fact, the level density approaches the well-known $\exp(a\sqrt{E})$, but this is of no concern in this paper.

The number of principal components $(NPC)_E = (\sum_k |C_k^E|^4)^{-1}$ and localization length $l_h(E) = \exp[(S_E^{\text{info}})] / (0.48d)$ with $S_E^{\text{info}} = -\sum_k |C_k^E|^2 \ln |C_k^E|^2$ are measures of complexity of the eigenfunctions, where d is the dimension of the Hamiltonian matrix. Hereafter, for a comparison, $(NPC)_E$ is also normalized to unity by dividing with the GOE value of $d/3$ and it is called $(RNPC)_E$; note that l_h is 1 for GOE. EGOE(1+2) in the Gaussian domain predicts [17]

$$(RNPC)_E = \sqrt{1 - \zeta^4} \exp\left(-\frac{\zeta^2 \hat{E}^2}{1 + \zeta^2}\right),$$

$$l_h(E) = \sqrt{1 - \zeta^2} \exp\left(\frac{\zeta^2}{2}\right) \exp\left(-\frac{\zeta^2 \hat{E}^2}{2}\right), \quad (3)$$

$$\zeta = \sqrt{1 - \sigma_k^2 / \sigma_H^2},$$

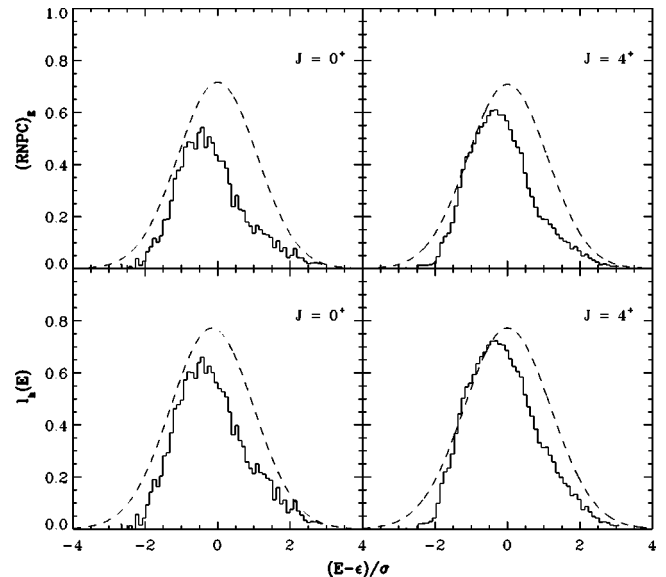


FIG. 4. Normalized number of principal components $(RNPC)_E$ and $l_h(E)$ compared with the TBRE predicted values given by Eq. (3). The histogram gives the calculated values and the dashed curve is the TBRE.

where $\overline{\sigma_k^2} = (1/d) \sum_{i \neq j} H_{ij}^2$ and $\sigma_H^2 = (1/d) \sum_i (E_i - \epsilon)^2$ are the variance of the off-diagonal Hamiltonian matrix elements and eigenvalues, respectively, see Ref. [23] for $(NPC)_E$ in BW domain. As ζ in Eq. (3) varies from 0 to 1, the $(NPC)_E$ and l_h change from GOE value to complete localization value. A comparison of the calculated $(RNPC)_E$ and $l_h(E)$, and TBRE predicted values are shown in Fig. 4. The envelope of the $(RNPC)_E$ and $l_h(E)$ shows that the overall trends are in a good agreement with the TBRE predictions. The correlation coefficient $\zeta \sim 0.85$ for both $J=0^+$ and 4^+ . It is seen that there are deviations in the lower tail region and also for the eigenstates above the centroid. This indicates that the states are more localized than what TBRE predicts [note that GOE value for both $(RNPC)_E$ and $l_h(E)$ is 1]. The calculated results are much closer to TBRE as compared to GOE but at the same time several states exhibit much more localization than what TBRE gives. The source of this localization need to be understood.

A statistical analysis of Sm I eigenvalues and eigenfunctions for $J=0^+$ and $J=4^+$ states with large number of

CSF's showed for the first time that atoms with sufficiently large number of active electrons exhibit TBRE characteristics. The tails of $\rho^H(E)$, multi-modal forms of $F_k(E)$, and stronger localization (compared even to TBRE) in some of the eigenstates seen in the calculation may be partly due to truncation of the CSF basis and partly also due to the nature of interelectron interaction. The sources of the deviations from the TBRE are being studied further. Here partitioned EGOE (see Ref. [8]) may be relevant. Although the λ value of EGOE(1+2) that maps the Hamiltonian (1) is not determined in this paper, it is established that the λ value exceeds λ_{F_k} as the Gaussian domain results are seen in Sm I, whereas Ce I and Pr I exhibits BW features [4,6]. We plan to carry out studies of Nd I and Pm I to establish BW to Gaussian transition with the increase of active electrons among the rare earth elements.

One of the authors (D.A.) would like to thank Vijay Sheorey for the useful discussions. All the calculations presented in the paper were carried out on an IBM-SP machine.

-
- [1] T.A. Brody, J. Flores, J.B. French, P.A. Mello, A. Pandey, and S.S.M. Wong, *Rev. Mod. Phys.* **53**, 385 (1981); F. Haake, *Quantum Signatures of Chaos*, 2nd ed. (Springer, New York, 2000); T. Guhr, A. Müller-Groeling, and H.A. Weidenmüller, *Phys. Rep.* **299**, 189 (1998).
- [2] N. Rosenzweig and C.E. Porter, *Phys. Rev.* **120**, 1698 (1960).
- [3] H.S. Camarda and P.D. Geogopoulos, *Phys. Rev. Lett.* **50**, 492 (1983).
- [4] V.V. Flambaum, A.A. Gribakina, G.F. Gribakin, and M.G. Kozlov, *Phys. Rev. A* **50**, 267 (1994).
- [5] V.V. Flambaum, A.A. Gribakina, G.F. Gribakin, and I.V. Ponomarev, *Physica D* **131**, 205 (1999).
- [6] A. Cummings, G. O'Sullivan, and D.M. Heffernan, *J. Phys. B* **34**, 3447 (2001).
- [7] A. Cummings, G. O'Sullivan, and D.M. Heffernan, *J. Phys. B* **34**, 3407 (2001).
- [8] V.K.B. Kota, *Phys. Rep.* **347**, 223 (2001).
- [9] Y. Alhassid, *Rev. Mod. Phys.* **72**, 895 (2000); Ph. Jacquod and A.D. Stone, *Phys. Rev. Lett.* **84**, 3938 (2000); *Phys. Rev. B* **64**, 214416 (2001); T. Papenbrock, L. Kaplan, and G.F. Bertsch, *ibid.* **65**, 235120 (2002); V.K.B. Kota and K. Kar, *Phys. Rev. E* **65**, 026130 (2002).
- [10] Y. Alhassid, Ph. Jacquod, and A. Wobst, *Phys. Rev. B* **61**, R13 357 (2000); Y. Alhassid and A. Wobst, *ibid.* **65**, 041304 (2002).
- [11] B. Georgeot and D.L. Shepelyansky, *Phys. Rev. E* **62**, 3504 (2000); **62**, 6366 (2000); G.P. Berman, F. Borgonovi, F.M. Izrailev, and V.I. Tsifrinovich, *ibid.* **65**, 015204 (2001); V.V. Flambaum and F.M. Izrailev, *ibid.* **64**, 026124 (2001).
- [12] F. Parpia, C. Fischer, and I. Grant, *Comput. Phys. Commun.* **94**, 249 (1996).
- [13] C. F. Froese Fischer, T. Brage, and P. Jansson, *Computational Atomic Structure: An MCHF Approach*, (Institute of Physics, Berkshire, 1997); H. Friederich, *Theoretical Atomic Physics* (Springer-Verlag, Berlin, 1998).
- [14] Angom Dilip, *et al.*, *Eur. Phys. J. D* **14**, 271 (2001); S.G. Porsev, *Phys. Rev. A* **56**, 3535 (1997).
- [15] K.K. Mon and J.B. French, *Ann. Phys. (N.Y.)* **95**, 90 (1975); L. Benet, T. Rupp, and H.A. Weidenmüller, *ibid.* **292**, 67 (2001).
- [16] Ph. Jacquod and D.L. Shepelyansky, *Phys. Rev. Lett.* **79**, 1837 (1997).
- [17] V.K.B. Kota and R. Sahu, *Phys. Rev. E* **64**, 016219 (2001).
- [18] V.V. Flambaum and F.M. Izrailev, *Phys. Rev. E* **61**, 2539 (2000).
- [19] Ph. Jacquod and I. Varga, *Phys. Rev. Lett.* **89**, 134101 (2002).
- [20] M.G. Kendall and A. Stuart, *Advanced Theory of Statistics*, 3rd ed. (Hafner, New York, 1969), Vol. 1.
- [21] L. Benet and H.A. Weidenmüller, e-print cond-mat/0207656; J. Flores, M. Horoi, M. Müller, and T.H. Seligman, *Phys. Rev. E* **63**, 026204 (2000).
- [22] G. O'Sullivan, P.K. Carroll, P. Dunne, R. Faulkner, C. McGuinness, and N. Murphy, *J. Phys. B* **32**, 1893 (1999).
- [23] In the BW domain, $(NPC)_E$ is $\pi\Gamma/2D(E)$ where $D(E)$ is the local mean spacing and Γ is the BW spreading width. This is used in Refs. [4–6] in the study of $(NPC)_E$ in Ce I and Pr I.